Optimization of computational ghost imaging

Chao Gao,[1] Xiaoqian Wang,[1,*] Zhifeng Wang,[1] Zhe Li,[2] Guijiao Du,[1] Feng Chang,[1] and Zhihai Yao[1,†]

[1]*Department of Physics, Changchun University of Science and Technology, Changchun 130022, People's Republic of China*

[2]*Department of Applied Mathematics, Changchun University of Science and Technology, Changchun 130022, People's Republic of China*

(Received 3 May 2017; published 15 August 2017)

We studied the second-order correlation function of computational ghost imaging, and we gave the expressions of second-order correlation function in the signal and background region. We found the total intensity of the modulated source influences the visibility of the reconstructed image. We discussed the positive-negative correlation phenomenon in a computational ghost imaging (CGI) system, and a protocol was given to distinguish the positive and negative correlations. This protocol allows us to determine the dividing line of positive and negative correlations before sampling, and it was verified by our simulations and experiments; the imaging quality of computational ghost imaging can be greatly improved by using this protocol.

DOI: 10.1103/PhysRevA.96.023838

I. INTRODUCTION

Ghost imaging is a novel technique which is based on the intensity correlation measurements. In the conventional ghost imaging system, a beam emitted by the light source is split into two equal beams, which travel along different optical paths: the signal and reference beam. The signal beam transmit through an object and its total intensity is measured by a bucket detector without any spatial resolution. The reference beam does not interact with the object and its intensity distribution is measured by a spatial-resolution detector. The image of the object is retrieved by the correlation measurement of the intensity at the two detectors. Ghost imaging was first proposed theoretically and performed experimentally with entangled photons [1,2]. Later, it was shown theoretically and experimentally that ghost imaging could be realized with a classical thermal light source [3–16]. Ghost imaging displays great potentials because of high lateral resolution imaging [17] and the resistant of atmosphere turbulence [18,19]. Due to these advantages of ghost imaging, how to effectively improve the imaging quality of ghost imaging has become a focus of study [20].

Later in 2008, Shapiro *et al.* proposed a computational ghost imaging (CGI) scheme [21] performed experimentally by Bromberg *et al.* [22]. The appearance of this ghost imaging scheme brought a debate about the physics of ghost imaging [21,23–25]. For a CGI system, it can create deterministic illumination patterns at the object position, then the reference beam becomes obsolete, and only a single pixel detector is needed. Comparing to conventional ghost imaging, the experimental setup of CGI is simpler. CGI has previously been performed by using a programable spatial light modulator (SLM) and a laser, and it can also be achieved by using a digital light projector. Having benefited from the usage of a programable light source, CGI opens the door for more advanced computational image reconstruction technique. A number of sophisticated algorithms have been developed over the years to improve the imaging quantity for a CGI system, such as differential computational ghost imaging (DCGI) [26], compressive sensing computational ghost imaging (CSCGI) [27], and so on [28–32].

Recently, Wu *et al.* proposed an imaging scheme based on conventional ghost imaging, in which a positive and negative image is reconstructed by conditional averaging of reference detector intensity [15]. Shih *et al.* provided a simple model of quantum interference to explain the positive-negative correlations in ghost imaging [33], then, they introduced the positive-negative-fluctuation-coincidence (PNFC) protocol to distinguish positive and negative correlations in ghost imaging [34]. By using this protocol, the imaging quality can be considerable improved.

In this paper, we consider a simple CGI system in which the source is modulated into a series of binary patterns with a deterministic black to white ratio, the second-order correlation function of this system is studied in Sec. II, and we give the expressions of the second-order correlation function for the signal and background region. By using these expressions, the visibility of the image reconstructed by the CGI system is investigated in Sec. III. Both the theoretical and experimental results show that we can get a reconstructed image with higher visibility by using binary patterns with lower proportion of white pixels. In Sec. IV, the positive-negative correlation phenomenon in our CGI system is discussed, and we give a protocol to distinguish the positive-negative correlations. This protocol is verified by our simulations and experiments, and we make a comparison with PNFC protocol in our CGI system. The results show that the criterion to distinguish the positive and negative correlations which are given by these two protocols approach to the same after a few measurements. The conclusions are finally given in Sec. V.

II. THE SECOND-ORDER CORRELATION FUNCTION IN THE SIGNAL AND BACKGROUND REGION

Figure 1 is the experimental setup for a CGI system. A series of binary patterns $R_n(i,j)$ are generated by computer. For each pattern, it is projected by a projector and illuminates the object, then the transmitted light is collected by a bucket detector. After K measurements, the image could be reconstructed by calculating the second-order correlation function [35]

$$G(i,j) = \frac{1}{K}\sum_{n=1}^{K} R_n(i,j)B_n, \tag{1}$$

*xqwang21@163.com
†yaozh@cust.edu.cn

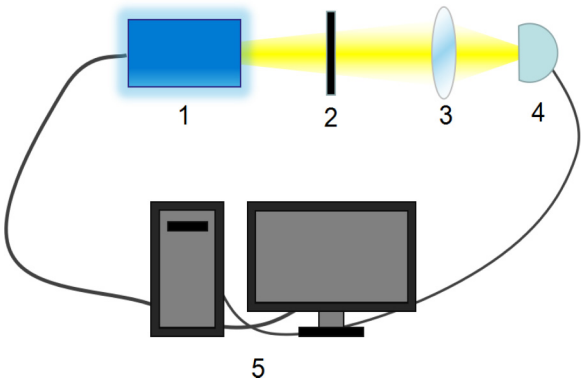

FIG. 1. Experimental setup of CGI. (1) Projector. (2) Transmissive object. (3) Collecting lens. (4) Bucket detector. (5) PC.

where B_n is the output of the bucket detector for each pattern $R_n(i,j)$, which is called the bucket signal in the following part of this paper.

In this paper, we consider the following assumptions:

(1) All the computer-generated binary patterns $R_n(i,j)$ have a deterministic white number α, and the amount of pixels in every pattern remains the same M.

(2) The binary patterns are independent of each other, and the set of the patterns is complete.

(3) The transmissive object is a pixelated object, and its transmission function $T(i,j)$ is binary distributed, with β transparent pixels.

In the following parts, we use a vector-matrix notation with $N_1 \times N_2$ patterns given as vectors in $\mathbb{C}^M$ which $M = N_1 N_2$, where $\mathbb{C}^M$ stands for the space of binary-valued vector of length M. These vectors are obtained from the standard matrix representation for the binary patterns by concatenating the columns of these matrices. Thus, the vectorial form of the second-order correlation function could be written as

$$\mathbf{G}(\xi) = \frac{1}{K}\sum_{n=1}^{K}\mathbf{R}_n(\xi)B_n. \tag{2}$$

Here, we consider the set of the patterns is complete, then, the number of total measurements $K = C_M^\alpha$, where $C_M^\alpha = \frac{M!}{\alpha!(M-\alpha)!}$ is the combination. B_n is the bucket signal which

$$B_n = \sum_{\xi_0=1}^{M}\mathbf{R}_n(\xi_0)\mathbf{T}(\xi_0)\,. \tag{3}$$

B_n could only be non-negative integers and the range of its value could be given by

$$B_n \in [\max(\alpha+\beta-M,0), \min(\alpha,\beta)]. \tag{4}$$

While the binary patterns illuminate the object, some of them may return the same bucket signal. That means in CGI, every bucket signal B_n may be corresponding to a lot of different binary patterns. Considering the bucket signal B_n has S different values in total, let B represent the set of the possible values of the bucket signal

$$B = \{B^{(1)}, B^{(2)}, B^{(3)}, \ldots, B^{(S)}\}. \tag{5}$$

In order to combine the similar terms, we divided the set of vector $\mathbf{R}_n$ in S subsets according to the bucket signal of each binary pattern.

$$R = \{R^{(1)}, R^{(2)}, R^{(3)}, \ldots, R^{(S)}\}, \tag{6}$$

where R is the set of vector R_n and $R^{(\zeta)}$ is a subset of R which every vector in $R^{(\zeta)}$ has the same bucket signal $B^{(\zeta)}$, so that Eq. (2) could also be written as

$$\mathbf{G}(\xi) = \frac{1}{K}\sum_{\zeta=1}^{S}B^{(\zeta)}\sum_{\eta=1}^{k^{(\zeta)}}\mathbf{R}^{(\zeta,\eta)}(\xi), \tag{7}$$

where $\mathbf{R}^{(\zeta,\eta)}$ is the ηth vector in subset $R^{(\zeta)}$. $k^{(\zeta)}$ is the number of the vectors in subset $R^{(\zeta)}$. When the set of the binary patterns is complete, $k^{(\zeta)}$ could be given by

$$k^{(\zeta)} = C_\beta^{B^{(\zeta)}} C_{M-\beta}^{\alpha-B^{(\zeta)}}. \tag{8}$$

According to the distribution of the object, we divide $\mathbf{R}^{(\zeta,\eta)}$ and $\mathbf{G}$ into two regions. We determine whether the pixels of the object are transparent or nontransparent. For those transparent pixels, let ξ_m represent their positions, where $m = 1,2,3,\ldots,\beta$, and let τ_n represent the positions of those nontransparent pixels, where $n = 1,2,3,\ldots,M-\beta$. We define $\mathbf{R}_s^{(\zeta,\eta)} = (\mathbf{R}^{(\zeta,\eta)}(\xi_1), \mathbf{R}^{(\zeta,\eta)}(\xi_2), \ldots, \mathbf{R}^{(\zeta,\eta)}(\xi_\beta))$ as the signal region of $\mathbf{R}^{(\zeta,\eta)}$, and $\mathbf{R}_b^{(\zeta,\eta)} = (\mathbf{R}^{(\zeta,\eta)}(\tau_1), \mathbf{R}^{(\zeta,\eta)}(\tau_2), \ldots, \mathbf{R}^{(\zeta,\eta)}(\tau_{M-\beta}))$ as the background region of $\mathbf{R}^{(\zeta,\eta)}$. The same method is used to define the signal and background region of $\mathbf{G}$.

Next, we discuss the value of second-order correlation function for the signal region. For vector $\mathbf{R}^{(\zeta,\eta)}$ with bucket signal of $B^{(\zeta)}$, $\mathbf{R}_s^{(\zeta,\eta)}$ has $C_\beta^{B^{(\zeta)}}$ different forms, and every form repeats $C_{M-\beta}^{\alpha-B^{(\zeta)}}$ times; that is because for every $\mathbf{R}_s^{(\zeta,\eta)}$, the corresponding $\mathbf{R}_b^{(\zeta,\eta)}$ has $C_{M-\beta}^{\alpha-B^{(\zeta)}}$ different forms in total. That means in the signal region, there are $C_\beta^{B^{(\zeta)}} C_{M-\beta}^{\alpha-B^{(\zeta)}}$ short vectors, which contain $C_{M-\beta}^{\alpha-B^{(\zeta)}}$ complete sets of combination $C_\beta^{B^{(\zeta)}}$. We can obtain

$$\begin{aligned}\sum_{\eta=1}^{k^{(\zeta)}}\sum_{m=1}^{\beta}\mathbf{R}^{(\zeta,\eta)}(\xi_m) &= \sum_{\eta=1}^{k^{(\zeta)}}\sum_{m=1}^{\beta}\mathbf{R}_s^{(\zeta,\eta)}(m)\\ &= B^{(\zeta)} C_\beta^{B^{(\zeta)}} C_{M-\beta}^{\alpha-B^{(\zeta)}}.\end{aligned} \tag{9}$$

For a complete vector set, the elements in it are uniformly distributed; we can obtain

$$\sum_{\eta=1}^{k^{(\zeta)}}\mathbf{R}^{(\zeta,\eta)}(\xi_m) = \frac{1}{\beta}B^{(\zeta)} C_\beta^{B^{(\zeta)}} C_{M-\beta}^{\alpha-B^{(\zeta)}}. \tag{10}$$

Substituting Eq. (10) into Eq. (7), we found that the result of the second-order correlation function in every position of the signal region is the same, namely

$$\begin{aligned} g_s &= \mathbf{G}(\xi_m)\\ &= \frac{1}{\beta K}\sum_{\zeta=1}^{S}(B^{(\zeta)})^2 C_\beta^{B^{(\zeta)}} C_{M-\beta}^{\alpha-B^{(\zeta)}}.\end{aligned} \tag{11}$$

Similarly, we can obtain the value of second-order correlation function for the background region

$$g_b = \mathbf{G}(\tau_n) = \frac{1}{(M-\beta)K}\sum_{\zeta=1}^{S} B^{(\zeta)}(\alpha - B^{(\zeta)})C_{\beta}^{B^{(\zeta)}} C_{M-\beta}^{\alpha-B^{(\zeta)}}. \quad (12)$$

Obviously, the value of the second-order correlation function in the signal region and the value of the background region are different. As a result, the object and the background are distinguished, so that the image of the object is reconstructed.

III. VISIBILITY OF CGI SYSTEM WITH DIFFERENT BINARY PATTERNS

We use the visibility to describe the imaging quality of CGI; it is usually defined as [11,12]

$$V = \frac{\langle G_{\text{in}}\rangle - \langle G_{\text{out}}\rangle}{\langle G_{\text{in}}\rangle + \langle G_{\text{out}}\rangle}, \quad (13)$$

where $\langle G_{\text{in}}\rangle$ and $\langle G_{\text{out}}\rangle$ are the average values of second-order correlation function in the signal region and background region, respectively. In our theory, the value of the second-order correlation function in every position of the signal region is a certain value g_s, and the value of the second-order correlation function in every position of the background region is a certain value g_b, and we can obtain that $\langle G_{\text{in}}\rangle = g_s$, $\langle G_{\text{out}}\rangle = g_b$. Thus, the visibility of the reconstructed image could be given by

$$V = \frac{|g_s - g_b|}{g_s + g_b}. \quad (14)$$

We studied the visibility of CGI when we use different binary patterns. We used binary patterns with different amount of white pixels and calculated the visibility in every situation. We also considered the visibility of CGI when the total number of the pixels in the binary patterns changes.

Figure 2 is the theoretical result of the visibility of CGI with different α/M. Parameter α/M is the proportion of the white pixels in the binary patterns; the value of α/M gets higher when we use binary patterns with more white pixels. In Figs. 2(a) and 2(b), we found that the visibility of CGI is decreasing when α/M increases. We also found that the visibility is also decreasing when M increases. For the same object, the visibility of the reconstructed image decreases when the imaging resolution increases, and vice versa. Comparing Figs. 2(a) with 2(b), we found that the visibility decreases when the object has more transparent pixels.

After all, in a CGI system, we can improve the visibility of the reconstructed image by decreasing the resolution of the binary patterns or decreasing the amount of white pixels of the binary patterns.

Figure 3 is the experimental result of images reconstructed by CGI with different α/M. The object is a binary transmitting object with the total transmissivity $\beta/M = 0.2400$, the total number of measurements $K = 20000$. In order to get a clearer view, for every reconstructed image, we use $G_I = G/G_{\min}$ to normalize the data of the second-order correlation function,

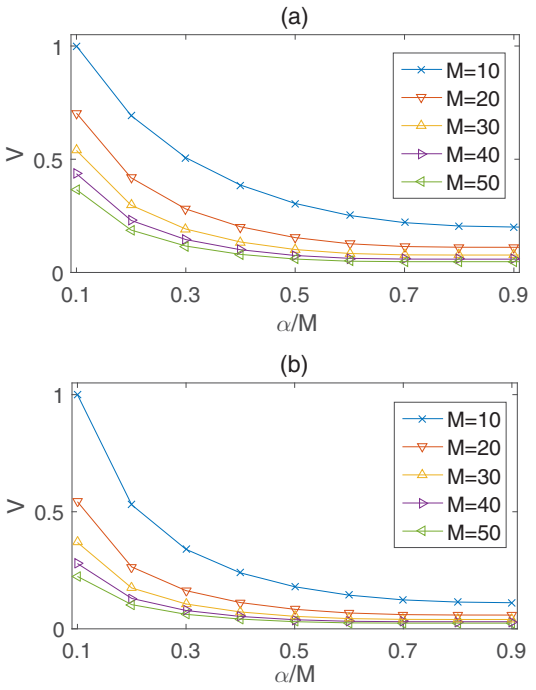

FIG. 2. Theoretical results of the visibility of CGI with different α/M. α/M is the proportion of the white pixels in the binary patterns. M is the amount of pixels in every binary pattern. β/M is the object's total transmission ratio, for (a) $\beta/M = 0.2$, and for (b) $\beta/M = 0.4$.

otherwise, the reconstructed images (a)–(h) are scaled into interval [1,1.2005]. The visibility of the reconstructed image is shown in Fig. 4; according to Fig. 4, it is clear that the visibility of the reconstructed image will be improved when we use binary patterns with a lower proportion of white pixels to illuminate the object.

IV. THE POSITIVE-NEGATIVE CORRELATION PHENOMENON IN A CGI SYSTEM

Since we obtained the expressions of the second-order correlation function in the signal and background region, the existence of the positive-negative correlation phenomenon in a CGI system can be inferred theoretically with these results.

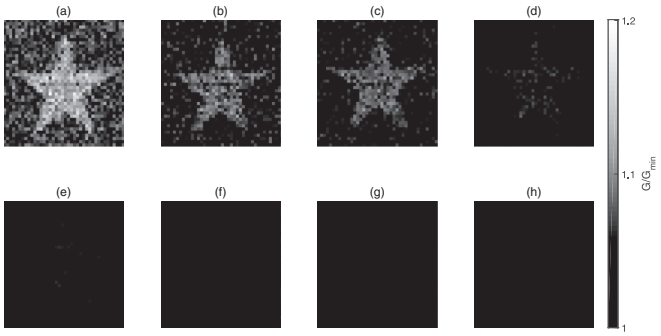

FIG. 3. Experiment result of images reconstructed by CGI with different α/M. From (a) to (h), the values of α/M are 0.125, 0.1875, 0.25, 0.375, 0.5, 0.625, 0.75, 0.875, respectively.

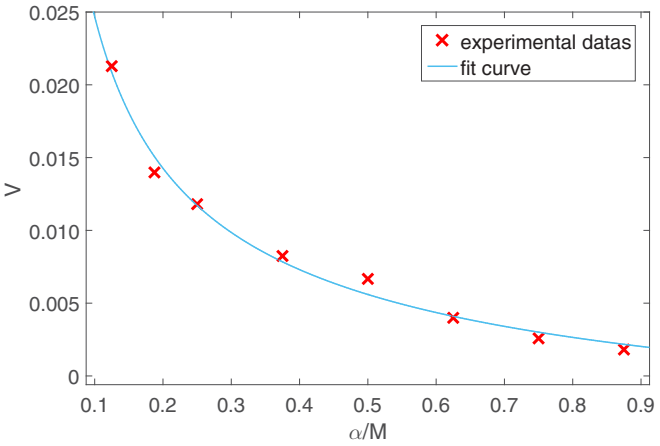

FIG. 4. The visibility of the reconstructed images in Figs. 3(a)–3(h).

Comparing g_s with g_b

$$\Delta G = g_s - g_b = \frac{\gamma}{K}\sum_{\zeta=1}^{S} C_{\beta}^{B^{(\zeta)}} C_{M-\beta}^{\alpha-B^{(\zeta)}} B^{(\zeta)}(M B^{(\zeta)} - \alpha\beta), \quad (15)$$

where $\gamma = \frac{1}{\beta(M-\beta)}$. Because α, β, M, $B^{(\zeta)}$ are non-negative integers, $\frac{\gamma}{K}$ and $C_{\beta}^{B^{(\zeta)}} C_{M-\beta}^{\alpha-B^{(\zeta)}}$ in Eq. (15) are positive. $B^{(\zeta)}(M B^{(\zeta)} - \alpha\beta)$ follows a parabola about $B^{(\zeta)}$. We divide all the correlation steps into 2 groups:

(1) Correlation steps with bucket signal $B^{(\zeta)} < \alpha\beta/M$.

(2) Correlation steps with bucket signal $B^{(\zeta)} > \alpha\beta/M$.

Normally, for the reconstructed image of the object, the values of the second-order correlation function in the signal region should be bigger than those pixels in the background region. However, if we superpose those correlation steps in group (1), the value of the second-order correlation function in the signal region will be smaller than the value in the background region; the signal to noise ratio of the reconstructed image is negative in this situation. Intuitively, that will cause the reverse of the grayscale of the reconstructed image and create a negative image of the object. We call these correlation steps as the "negative correlations," and the rest of the correlation steps as the "positive correlations."

It is clear that we can distinguish the positive and negative correlations by judging the values of the bucket signals. The criterion to distinguish the positive and negative correlations is $\alpha\beta/M$; we define it as the "reverse factor:"

$$RF = \frac{\alpha\beta}{M}. \quad (16)$$

We can find that RF is related with β/M and α, which are the transmission ratio of the object and the number of the white pixels in each binary pattern.

Shih *et al.* also gave a protocol to distinguish the positive-negative correlations, which use the mean of the bucket signal as the criterion to distinguish the positive and negative correlations. We make a comparison between PNFC protocol and our protocol in our CGI system. We choose a 20×20 binary picture with 117 transparent pixels as the object (where $\frac{\beta}{M} = \frac{117}{400}$), and 10^5 random binary patterns with $\alpha = 100$ to illuminate the object.

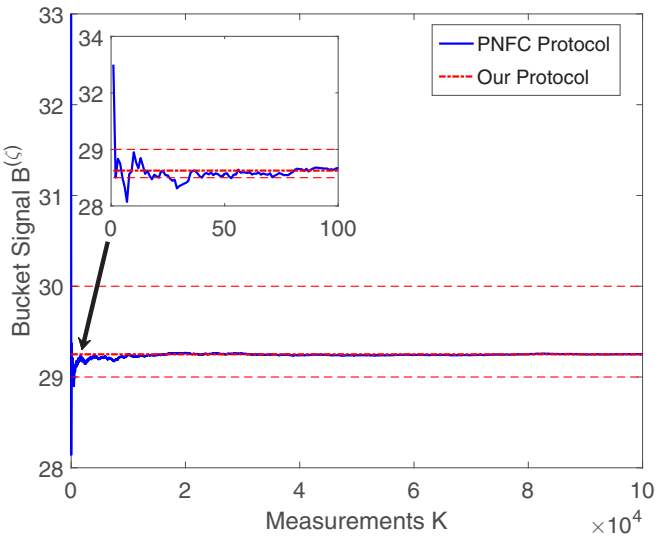

FIG. 5. Comparison of the criterion to distinguish positive and/or negative correlations determined by PNFC protocol and our protocol. The criterion determined by our protocol is 29.25; the two dashed lines are 29 and 30, respectively.

Figure 5 shows the result of the comparison between the dividing line given by PNFC protocol and our protocol. Notice that the bucket signal can only be integers; the values in the interval (29,30] actually have the same effect. After several measurements, the criterion determined by these two methods approach to the same. However, by using our protocol, the transmitting ratio of the object is measurable, and the number of the white pixels in the binary patterns is known, thus we are able to determine the criterion up front before sampling;

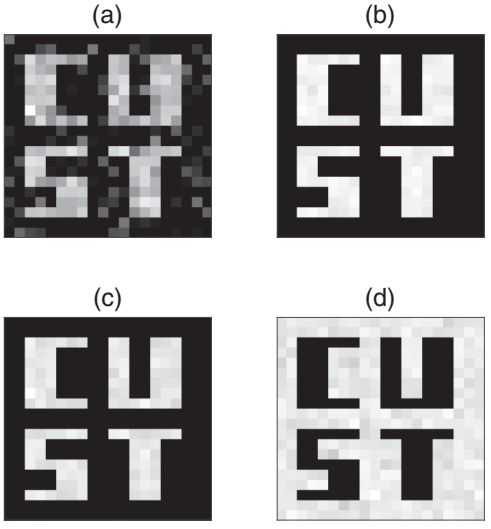

FIG. 6. Simulation results of positive-negative correlation in a CGI system. (a) The reconstructed image of CGI. (b) The reconstructed image when we reverse the negative correlation steps. (c) The positive image. (d) The negative image.

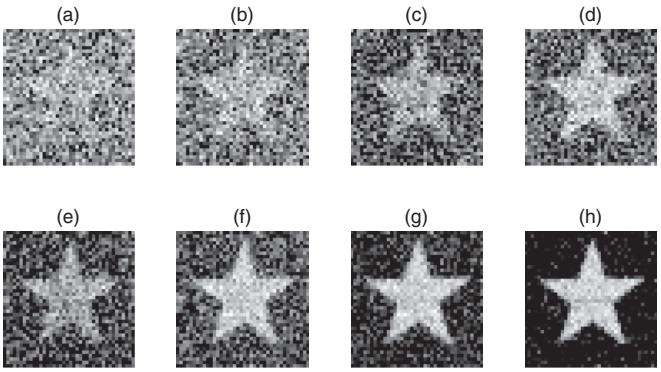

FIG. 7. Experimental results of conventional CGI versus CGI reversing the negative image. (a)–(d) are the reconstructed images of normal CGI, and (e)–(h) are the reconstructed images of CGI reversing the grayscale of negative correlation steps. The numbers of total measurements of (a) and (e), (b) and (f), (c) and (g), (d) and (h) are 2000, 5000, 10 000, 20 000, respectively.

it is more convenient to separate the positive and negative correlations while sampling.

Now, we are able to separate negative correlations from the whole sampling data by using RF. In the following simulations and experiments, we use reverse factor RF to distinguish the positive and negative correlations. Figure 6 shows the results of the simulation for positive-negative correlation in a CGI system. Comparing Figs. 6(a) with 6(b), we find that in CGI, when we reverse the grayscale of the negative correlations, the quality of the reconstructed image will be considerably improved.

Figure 7 shows the result of our experiment for comparing CGI with CGI reversing the negative correlations. In our experiment, the object is a 7 mm $\times$ 7 mm binary transmitting object with the transmission ratio $\beta/M = 0.2400$. We use a series of 40×40 random binary patterns as the source; each of them has 1400 white pixels ($\alpha = 1400$). Comparing Figs. 7(a)–7(d) with Figs. 7(e)–7(h), for the same number of measurements, the quality of the reconstructed images are much better when we reverse the grayscale of the negative correlations.

V. CONCLUSIONS

In this paper, we studied the second-order correlation function of a CGI system, and we gave the expressions for the second-order correlation function in the signal and background regions, respectively. According to our theory, we found the visibility is influenced by the proportion of white pixels in the binary patterns: The visibility of the reconstructed image could be improved when we use binary patterns with a lower proportion of white pixels. Otherwise, from the expressions of second-order correlation function in signal and background regions, it is found that the positive-negative correlations in a CGI system also exist. According to our theory, whether the current step is a positive or negative correlation lies on the value of its bucket signal; the dividing line is the product of the object's transmission/reflection ratio and the intensity of the source. For a negative (positive) correlation, the value of the corresponding bucket signal is below (above) the dividing line, and this protocol is verified by our simulations and experiments. Furthermore, by using our protocol, we are able to determine the dividing line up front. Thus it is possible to separate the positive and/or negative correlations in the process of sampling; we believe that this advantage will be helpful in practical applications. Grayscaled object could be regarded as the superposing of several binary objects, so that our theory could extend to the CGI with a grayscale object; we will discuss it in our further researches.

ACKNOWLEDGMENTS

This work is supported by the National Natural Science Foundation of China with Grants No. 11305020, No. 11647054, and No. 11601039. This work is also supported by the Science and Technology Research Projects of the Education Department of Jilin Province, China with Grant No. 2016-354.

[1] D. N. Klyshko, Phys. Lett. A **132**, 299 (1988).
[2] T. B. Pittman, Y. H. Shih, D. V. Strekalov, and A. V. Sergienko, Phys. Rev. A **52**, R3429(R) (1995).
[3] F. Ferri, D. Magatti, V. G. Sala, and A. Gatti, Appl. Phys. Lett. **92**, 261109 (2008).
[4] A. Gatti, M. Bache, D. Magatti, E. Brambilla, F. Ferri, and L. A. Lugiato, J. Mod. Opt. **53**, 739 (2006).
[5] R. S. Bennink, S. J. Bentley, and R. W. Boyd, Phys. Rev. Lett. **89**, 113601 (2002).
[6] A. Gatti, E. Brambilla, M. Bache, and L. A. Lugiato, Phys. Rev. Lett. **93**, 093602 (2004).
[7] A. Gatti, E. Brambilla, M. Bache, and L. A. Lugiato, Phys. Rev. A **70**, 013802 (2004).
[8] A. Valencia, G. Scarcelli, M. D'Angelo, and Y. Shih, Phys. Rev. Lett. **94**, 063601 (2005).
[9] K. W. C. Chan, M. N. O'Sullivan, and R. W. Boyd, Phys. Rev. A **79**, 033808 (2009).
[10] X.-H. Chen, Q. Liu, K.-H. Luo, and L.-A. Wu, Opt. Lett. **34**, 695 (2009).
[11] K. W. C. Chan, M. N. O'Sullivan, and R. W. Boyd, Opt. Express **18**, 5562 (2010).
[12] K. W. C. Chan, M. N. O'Sullivan, and R. W. Boyd, Opt. Lett. **34**, 3343 (2009).
[13] M.-J. Sun, M.-F. Li, and L.-A. Wu, Appl. Opt. **54**, 7494 (2015).
[14] S.-C. Song, M.-J. Sun, and L.-A. Wu, Opt. Commun. **366**, 8 (2016).
[15] L.-A. Wu and K.-H. Luo, AIP Conf. Proc. **1384**, 223 (2011).
[16] K.-H. Luo, B.-Q. Huang, W.-M. Zheng, and L.-A. Wu, Chin. Phys. Lett. **29**, 074216 (2012).
[17] W. Gong and S. Han, Phys. Lett. A **376**, 1519 (2012).
[18] P. B. Dixon, G. A. Howland, K. W. C. Chan, C. O'Sullivan-Hale, B. Rodenburg, N. D. Hardy, J. H. Shapiro, D. S. Simon, A. V. Sergienko, R. Boyd *et al.*, Phys. Rev. A **83**, 051803(R) (2011).

[19] R. E. Meyers, K. S. Deacon, and Y. Shih, Appl. Phys. Lett. **98**, 111115 (2011).
[20] F. Ferri, D. Magatti, L. A. Lugiato, and A. Gatti, Phys. Rev. Lett. **104**, 253603 (2010).
[21] J. H. Shapiro, Phys. Rev. A **78**, 061802(R) (2008).
[22] Y. Bromberg, O. Katz, and Y. Silberberg, Phys. Rev. A **79**, 053840 (2009).
[23] M. Bache, D. Magatti, F. Ferri, A. Gatti, E. Brambilla, and L. A. Lugiato, Phys. Rev. A **73**, 053802 (2006).
[24] G. Scarcelli, V. Berardi, and Y. Shih, Phys. Rev. Lett. **96**, 063602 (2006).
[25] R. Meyers, K. S. Deacon, and Y. Shih, Phys. Rev. A **77**, 041801(R) (2008).
[26] B. Sun, M. Edgar, R. Bowman, L. Vittert, S. Welsh, A. Bowman, and M. Padgett, in *Computational Optical Sensing and Imaging* (Optical Society of America, Arlington, Virginia, 2013), p. CTu1C.4.
[27] V. Katkovnik and J. Astola, J. Opt. Soc. Am. A **29**, 1556 (2012).
[28] B. Sun, M. P. Edgar, R. Bowman, L. E. Vittert, S. Welsh, A. Bowman, and M. Padgett, Science **340**, 844 (2013).
[29] P. Clemente, V. Durán, V. Torres-Company, E. Tajahuerce, and J. Lancis, Opt. Lett. **35**, 2391 (2010).
[30] N. D. Hardy and J. H. Shapiro, Phys. Rev. A **87**, 023820 (2013).
[31] M. Tanha, R. Kheradmand, and S. Ahmadi-Kandjani, Appl. Phys. Lett. **101**, 101108 (2012).
[32] B. I. Erkmen, J. Opt. Soc. Am. A **29**, 782 (2012).
[33] R. E. Meyers, K. S. Deacon, and Y. Shih, Appl. Phys. Lett. **100**, 131114 (2012).
[34] H. Chen, T. Peng, and Y. Shih, Phys. Rev. A **88**, 023808 (2013).
[35] M. O. Scully and M. S. Zubairy, in *Quantum Optics* (Cambridge University Press, New York, 1997), p. 630.